

Increased Respiration in the *sch9*Δ Mutant Is Required for Increasing Chronological Life Span but Not Replicative Life Span[∇]

Hugo Lavoie and Malcolm Whiteway*

*Biotechnology Research Institute, National Research Council, Montreal, Quebec H4P 2R2, and
Department of Biology, McGill University, Montreal Quebec, H3A 1B1, Canada*

Received 4 September 2007/Accepted 28 April 2008

Loss of the protein kinase Sch9p increases both the chronological life span (CLS) and the replicative life span (RLS) of *Saccharomyces cerevisiae* by mimicking calorie restriction, but the physiological consequences of *SCH9* deletion are poorly understood. By transcriptional profiling of an *sch9*Δ mutant, we show that mitochondrial electron transport chain genes are upregulated. Accordingly, protein levels of electron transport chain subunits are increased and the oxygen consumption rate is enhanced in the *sch9*Δ mutant. Deletion of *HAP4* and *CYT1*, both of which are essential for respiration, revert the *sch9*Δ mutant respiratory rate back to a lower-than-wild-type level. These alterations of the electron transport chain almost completely blocked CLS extension by the *sch9*Δ mutation but had a minor impact on the RLS. *SCH9* thus negatively regulates the CLS and RLS through inhibition of respiratory genes, but a large part of its action on life span seems to be respiration independent and might involve increased resistance to stress. Considering that *TOR1* deletion also increases respiration and that Sch9p is a direct target of TOR signaling, we propose that *SCH9* is one of the major effectors of TOR repression of respiratory activity in glucose grown cells.

The *SCH9* gene of the yeast *Saccharomyces cerevisiae* encodes a serine-threonine protein kinase with a catalytic domain very similar to that of human AKT1 (12). This kinase participates in a conserved signaling network involving upstream acting kinases: Pkh1/2p, which phosphorylate its activation loop, and Tor1/2p, which target its hydrophobic motif (34, 36, 38).

There are several lines of evidence that Sch9p plays an important role in glucose signaling in the budding yeast. Early work showed parallelism and complementarity of *SCH9* signaling with the cyclic AMP-dependent protein kinase (PKA) pathway, which signals hexose abundance (25, 29, 37, 40). Overexpression of *SCH9* suppresses the growth defect of many PKA pathway component mutations (37), and the *sch9*Δ null mutant is synthetically lethal with each of *gpr1*Δ, *gpa2*Δ, and *ras2*Δ mutations, which act upstream of PKA (25, 29, 37). It was also recently shown that Sch9p integrates nutrient signals with cell size regulation. In fact, the *sch9*Δ mutation was one of the most potent modifiers of cell size identified in a genome-wide screen for pathways coupling cell growth and division in yeast (18). A subsequent study showed that Sch9p is an activator of ribosomal protein and ribosomal biogenesis regulons and is required for carbon source modulation of cell size (19).

SCH9 is also a negative regulator of both the chronological life span (CLS) and the replicative life span (RLS), both of which are influenced by glucose availability (12, 21, 22, 24). The CLS is the relative survival over time of yeast cells grown to stationary phase in liquid culture, while the RLS is defined as the number of daughter cells produced by a given yeast mother cell before senescence (11, 16, 21). In addition to the

*sch9*Δ deletion, targeting of either the TOR or cyclic AMP/PKA pathway also extends the CLS and RLS (12, 27, 33). As well as these genetic manipulations, calorie restriction (CR) lengthens the *S. cerevisiae* CLS and RLS (9, 17, 24, 27). Although this is currently controversial, respiration is suggested to be critical for the physiology of life span because (i) the effect of CR on the RLS is mimicked by overexpressing *HAP4*, which activates expression of electron transport chain genes and is blocked by deletion of *CYT1* (28), and (ii) affecting respiration by blocking mitochondrial transcription, ATP synthesis, or the electron transport chain (*atp2*Δ, *coq3*Δ, or *ndi1*Δ deletions or antimycin A treatment) causes a reduction of the yeast CLS (5, 10). *HAP4* overexpression also causes an increased CLS, suggesting that increasing respiration may promote RLS and CLS extension (32). Recently, it was convincingly shown that both the *sch9*Δ and the *tor1*Δ mutations mimic CR and that reduction in TOR signaling increases yeast respiratory activity (4, 24). However, the physiological effects of perturbing Sch9p signaling remain largely uncharacterized. Here we show that the *sch9*Δ mutation is required for a derepression of respiration in glucose-grown cells and that this causes part of the extended CLS and RLS phenotype of the *sch9*Δ mutant.

MATERIALS AND METHODS

Yeast strains and growth conditions. All *Saccharomyces cerevisiae* strains used in this study are BY4741 (*MATa his3Δ1 leu2Δ0 met15Δ0 ura3Δ0*) and its isogenic derivatives (39). The *sch9*Δ heterozygous mutant was provided by Mike Tyers (18). The *hap4*Δ and *cyt1*Δ mutants were obtained from the Research Genetics yeast knockout library (Research Genetics). Double mutants were generated by standard yeast genetic manipulations. All strains were cultivated in SD-complete containing 2% dextrose, following standard protocols (1). The plasmid pMT3569, encoding hemagglutinin-Sch9p was a gift of Mike Tyers (19). This construct was subjected to PCR site-directed mutagenesis to introduce a kinase-disabling mutation (K441A). Transformations were performed with the lithium acetate method (13).

* Corresponding author. Mailing address: 6100 Royalmount Ave., Montreal, Quebec H4P 2R2, Canada. Phone: (514) 496-6146. Fax: (514) 496-6213. E-mail: malcolm.whiteway@nrc-nrc.gc.ca.

[∇] Published ahead of print on 9 May 2008.

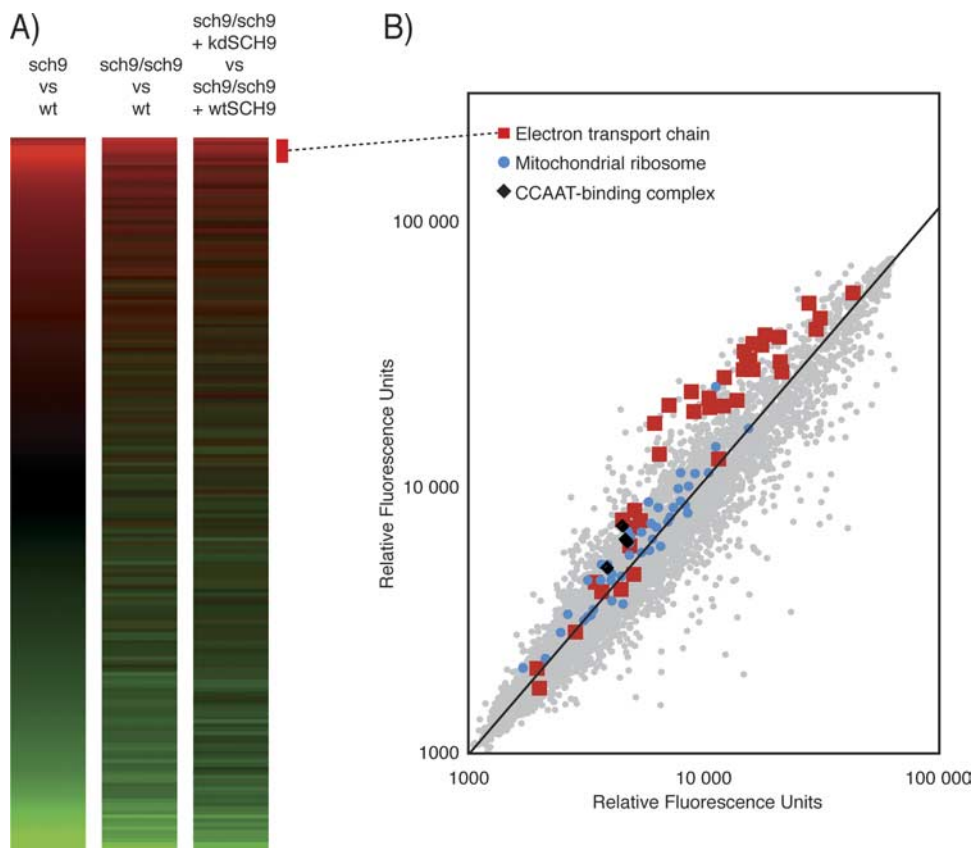


FIG. 1. Gene expression is massively affected by deletion of *SCH9*. (A) The transcription profile of the *sch9Δ* cells is reproducible in haploid, diploid, or transformed strains. wt, wild type. (B) Electron transport chain components, the mitochondrial ribosome, and the CCAAT box complex proteins are systematically upregulated in the *sch9Δ* mutant.

RNA extraction and labeling. All cultures used for RNA extractions were grown to an optical density at 600 nm OD_{600} of 1, and the glucose concentration in the medium was quantitated with a glucose assay kit (Sigma) to ensure that culture conditions were the same for all analyzed strains. Total RNA was extracted by the hot-phenol extraction method (6) with the difference that glass beads (Sigma) were added to samples. Poly(A)⁺ RNAs were purified using the Invitrogen MicroFast Track kit (Invitrogen). For labeling, 5 μ g of poly(A)⁺ RNA was reverse transcribed using oligo(dT)₂₁ in the presence of Cy3 or Cy5-dCTP (Perkin-Elmer-Cetus/NEN) and Superscript II reverse transcriptase (Invitrogen). Reverse transcription reaction mixtures were treated with a mix of RNase H (Sigma) and RNase A (1 mg/ml) for 15 min at 37°C. The labeled cDNAs were purified with the QIAquick PCR purification kit (Qiagen).

Microarray analysis. *Saccharomyces cerevisiae* Y6.4k cDNA arrays containing 6,218 genes printed in duplicate were obtained from University Health Networks (Toronto, Canada) and used for all hybridizations. The microarray slides were prehybridized for 2 h at 42°C with DIGeasy hybridization buffer containing yeast tRNA and salmon sperm DNA and subsequently washed with 0.1 \times SSC (1 \times SSC is 0.15 M NaCl plus 0.015 M sodium citrate) and air dried. The slides were then hybridized with labeled cDNAs overnight at 42°C in DIGeasy hybridization buffer with yeast tRNA and salmon sperm DNA. The slides were washed twice with SSC-0.2% sodium dodecyl sulfate (SDS), once with 0.1 \times SSC-0.2% SDS, and three times with 0.1 \times SSC. A final wash with isopropanol was performed, and slides were air dried and scanned with a ScanArray 5000 scanner (Perkin-Elmer-Cetus) at 10- μ m resolution. Signal intensity was quantified with QuantArray software (Perkin-Elmer-Cetus), and final normalization and inspection of the data were done with the GeneSpring package.

Southern and Northern blotting. DNA extracts used for Southern blotting were obtained by the rapid glass beads method (15). Genomic DNA was digested with HaeIII and run on a 1% agarose gel. DNA was then transferred by capillary action to a Zeta-Probe nylon membrane (Bio-Rad). To obtain Northern blots, total RNA (80 μ g) was electrophoresed on a 7.5% formaldehyde-1%

agarose gel and transferred by blotting to a Zeta-Probe nylon membrane (Bio-Rad).

Southern probes were a XbaI-PstI restriction fragment of the *ACT1* gene from plasmid pGEM-ACT1 (41) and a *COX2* probe generated by PCR. Northern probes were all generated by PCR. All probes were labeled by random priming with the RediPrime kit (Amersham Biosciences). Southern and Northern blot hybridizations were carried out as described previously (30).

Protein methods. Whole-cell extracts were obtained by bead beating in a buffer containing 0.1% NP-40, 250 mM NaCl, 50 mM NaF, 5 mM EDTA, and 50 mM Tris-HCl, pH 7.5. Complete protease inhibitor cocktail (Roche) was added just before use. Protein concentrations were determined by the standard Bio-Rad protein assay (Bio-Rad). Proteins were separated on a 10% SDS-polyacrylamide gel and transferred to a polyvinylidene difluoride membrane (Millipore). Antibodies were prepared in phosphate-buffered saline-0.05% Tween 20-5% skim milk powder. Rabbit polyclonal antibodies directed against Atp1p, Atp2p, and Atp7p were kind gifts of Jean Velours. They were used at dilutions of 1:100,000, 1:100,000 and 1:10,000, respectively. Antibodies directed against Cox4p, Cox5p, and Cyt1p were obtained from Alexander Tzagoloff and were all used at a dilution of 1:1000 (2). Horseradish peroxidase (HRP)-conjugated anti-rabbit and anti-mouse secondary antibodies (Santa Cruz) were used at 1:10,000. The HRP signal was revealed with Immobilon HRP substrate (Millipore).

Oxygen consumption measurements. Cells were grown to an OD_{600} of 1, spun down, and kept on ice. One hour before the measurements, cells were resuspended in SD-2% glucose and put on a shaker at 30°C for 1 hour. OD_{600} measurements and cell counts were performed immediately before putting cells in the oxygen sensing setup. The oxygen depletion rate was monitored by using a lab-built respirometer comprising a polarographic dissolved oxygen probe in a glass syringe with constant agitation (26). Oxygen consumption rates were expressed as percent O₂ per minute per 1×10^6 cells.

Microscopy. Wild-type or *sch9Δ* mutant cells expressing Cox4p-red fluorescent protein (RFP) (3) were stained with DAPI (4',6'-diamidino-2-phenylindole) (10

TABLE 1. GO term annotations that are significantly upregulated in the *sch9Δ* mutant ($P < 1 \times 10^{-4}$)

| GO category | GO no. | <i>P</i> value | GO description | |
|--------------------|--------------------|----------------|--|--|
| Biological process | GO:0006119 | 2.78E-15 | Oxidative phosphorylation | |
| | GO:0006118 | 3.12E-11 | Electron transport | |
| | GO:0042775 | 4.98E-11 | ATP synthesis-coupled electron transport (sensu Eukarya) | |
| | GO:0006122 | 6.49E-08 | Mitochondrial electron transport, ubiquinol to cytochrome <i>c</i> | |
| | GO:0006091 | 1.32E-07 | Energy pathways | |
| | GO:0045333 | 1.11E-06 | Cellular respiration | |
| | GO:0006754 | 5.44E-06 | ATP biosynthesis | |
| | GO:0016310 | 5.45E-06 | Phosphorylation | |
| | GO:0009206 | 1.59E-05 | Purine ribonucleoside triphosphate biosynthesis | |
| | GO:0009201 | 2.57E-05 | Ribonucleoside triphosphate biosynthesis | |
| | GO:0006796 | 8.63E-05 | Phosphate metabolism | |
| | GO:0006123 | 1.26E-04 | Mitochondrial electron transport, cytochrome <i>c</i> to oxygen | |
| | Cellular component | GO:0005746 | 3.79E-13 | Mitochondrial electron transport chain |
| | | GO:0005750 | 6.95E-09 | Respiratory chain complex III (sensu Eukarya) |
| GO:0005743 | | 9.42E-07 | Mitochondrial inner membrane | |
| GO:0005740 | | 5.05E-06 | Mitochondrial membrane | |
| GO:0005753 | | 5.44E-06 | Proton-transporting ATP synthase complex (sensu Eukarya) | |
| GO:0005751 | | 4.16E-05 | Respiratory chain complex IV (sensu Eukarya) | |
| GO:0016602 | | 8.98E-05 | cCAAT-binding factor complex | |
| Molecular function | | GO:0008121 | 6.49E-08 | Ubiquinol-cytochrome <i>c</i> reductase activity |
| | GO:0046933 | 2.72E-05 | Hydrogen-transporting ATP synthase activity, rotational mechanism | |
| | GO:0004129 | 4.16E-05 | Cytochrome <i>c</i> oxidase activity | |
| | GO:0015075 | 6.26E-05 | ion transporter activity | |

μg/ml in phosphate-buffered saline plus 2% glucose) for 10 min at room temperature, washed twice, and visualized with a Leica DM-IRE2 inverted microscope with a 63× objective and a 10× projection lens. Pictures were acquired with a Sensys charge-coupled-device camera. Images were manipulated with the Openlab software (Improvision).

Longevity analysis. CLS and RLS analyses were performed in YPD as described previously (10, 22). RLS differences from the wild-type control were tested using the Wilcoxon rank sum test (21).

RESULTS

The *sch9Δ* mutation upregulates electron transport chain gene expression. We profiled the *sch9Δ* mutant by microarray analysis in the haploid and diploid states (Fig. 1A). We also compared *sch9Δ/sch9Δ* diploid mutants transformed with a wild-type *SCH9* or a kinase-dead *SCH9* version (kd-*SCH9*; K441A). The profiles obtained are highly reproducible (Fig. 1A) and reveal that numerous genes are upregulated in the *sch9Δ* mutant (643 genes; $P < 0.05$). The list of upregulated genes was systematically tested for enrichment in gene ontology (GO) terms from the SGD database (<http://www.yeastgenome.org/>). A randomized set of GO annotations was used to set the threshold *P* value ($P < 1 \times 10^{-4}$). Most of the nonredundant GO terms significantly associated with the upregulated gene list are related to energy derivation and ATP synthesis (Table 1). The other GO terms are associated with chromatin organization and RNA polymerase II-dependent transcription. Genes involved in mitochondrial functions that are upregulated in the *sch9Δ* mutant are listed in Table 2 ($P < 0.05$). Almost all components of the five respiratory complexes are upregulated with fold changes that range from 1.2 to 2.5. In addition to canonical members of the respiratory complexes, cytochrome *c* oxidase chaperones (*PET100*, *PET191*, *COX14*, and *COX17*), heme biosynthesis enzymes (*HEM4*, *HEM12*, and *HEM15*), holocytochrome *c* synthases (*CYC3* and *CYT2*), and

mitochondrial ribosomal subunit genes are upregulated (Table 2; Fig. 1B). These observations suggest that the *sch9Δ* mutation affects respiratory physiology. We therefore decided to study the mitochondrial compartment of the *sch9Δ* mutant in more detail.

Increased respiration in the *sch9Δ* strain. The *sch9Δ* mutant has a slow-growth phenotype that is a hallmark of petite mutants. However, our *sch9Δ* strain could grow on ethanol, glycerol, pyruvate, and succinate as sole carbon sources, suggesting that it is not a petite (data not shown). Since *ABF2*, *MGM101*, *KGD2*, and *ACO1* are upregulated in the *sch9Δ* mutant (Table 2) and these genes are involved in mitochondrial DNA (mtDNA) maintenance, we also tested whether the *sch9Δ* mutant displays modified mtDNA abundance (7, 31, 35, 41). For this, Southern blot analysis with probes for a mitochondrial gene (*COX2*) and a single-copy nuclear gene (*ACT1*) was performed. As expected, the mtDNA/genomic DNA ratio increased as the culture density increased, but we observed no differences in mtDNA amounts between the *sch9Δ* mutant and the wild-type strain (Fig. 2A). We also microscopically examined the mitochondrial compartment in *sch9Δ* and observed that it is more densely stained and speckled than in wild-type cells, where DAPI staining and Cox4p-RFP distribution are diffuse and reticulated (Fig. 2B).

We validated that the increased expression of the respiratory regulon in *sch9Δ* cells corresponds to enhanced respiratory activity. First, Western blotting of cultures at different cell densities established that protein levels of Atp1p, Atp2p, Atp7p, Cox4p, Cox5p, and Cyt1p are higher in *sch9Δ* cells throughout culture growth (Fig. 3A). At all time points evaluated, glucose availability was the same in the wild-type and *sch9Δ* cultures (data not shown). Since the expression of electron transport chain mRNAs and proteins is increased in the

TABLE 2. Mitochondrial genes that are significantly upregulated in the *sch9Δ* mutant ($P < 0.05$)

| Function | Gene | | Increase in expression (fold) | <i>P</i> value |
|---|-----------------|---------------|-------------------------------|----------------|
| | Systematic name | Common name | | |
| Complex I | YML120C | <i>ND11</i> | 1.27 | 2.99E-02 |
| Electron transport chain complex II, succinate dehydrogenase | YKL148C | <i>SDH1</i> | 1.27 | 3.71E-02 |
| | YKL141W | <i>SDH3</i> | 1.65 | 1.33E-04 |
| | YDR178W | <i>SDH4</i> | 1.83 | 8.61E-07 |
| Electron transport chain complex III (GO:0005750), cytochrome <i>c</i> reductase | YBL045C | <i>COR1</i> | 1.66 | 8.72E-05 |
| | YHR001W-A | <i>QCR10</i> | 2.59 | 1.71E-05 |
| | YPR191W | <i>QCR2</i> | 1.60 | 2.63E-04 |
| | YFR033C | <i>QCR6</i> | 2.04 | 6.20E-07 |
| | YDR529C | <i>QCR7</i> | 2.03 | 1.62E-05 |
| | YJL166W | <i>QCR8</i> | 2.01 | 1.14E-06 |
| | YGR183C | <i>QCR9</i> | 1.48 | 2.43E-03 |
| | YEL024W | <i>RIP1</i> | 1.36 | 9.92E-03 |
| | YJR048W | <i>CYC1</i> | 1.89 | 1.11E-04 |
| | YAL039C | <i>CYC3</i> | 1.52 | 1.31E-03 |
| | YML054C | <i>CYB2</i> | 1.21 | 8.59E-03 |
| | YOR065W | <i>CYT1</i> | 1.92 | 7.83E-04 |
| | YKL087C | <i>CYT2</i> | 1.24 | 6.64E-03 |
| Electron transport chain complex IV (GO:0005751), cytochrome <i>c</i> oxidase | YGL191W | <i>COX13</i> | 1.88 | 5.54E-05 |
| | YML129C | <i>COX14</i> | 1.16 | 2.49E-02 |
| | YLL009C | <i>COX17</i> | 1.85 | 5.40E-04 |
| | YDR231C | <i>COX20</i> | 1.25 | 2.24E-03 |
| | YGL187C | <i>COX4</i> | 1.69 | 3.07E-05 |
| | YNL052W | <i>COX5A</i> | 1.79 | 1.27E-05 |
| | YHR051W | <i>COX6</i> | 1.92 | 1.45E-07 |
| | YMR256C | <i>COX7</i> | 2.42 | 3.69E-06 |
| | YLR395C | <i>COX8</i> | 1.89 | 7.15E-05 |
| | YDL067C | <i>COX9</i> | 1.58 | 2.85E-08 |
| | YDR079W | <i>PET100</i> | 1.54 | 8.61E-04 |
| YJR034W | <i>PET191</i> | 1.29 | 2.77E-02 | |
| Electron transport chain complex V (GO:0005753), F ₁ F ₀ ATP synthase | YBL099W | <i>ATP1</i> | 1.43 | 5.27E-03 |
| | YLR295C | <i>ATP14</i> | 1.96 | 1.11E-05 |
| | YPL271W | <i>ATP15</i> | 1.56 | 1.07E-02 |
| | YDL004W | <i>ATP16</i> | 1.74 | 4.45E-04 |
| | YDR377W | <i>ATP17</i> | 1.47 | 1.12E-03 |
| | YPR020W | <i>ATP20</i> | 2.61 | 1.10E-07 |
| | YBR039W | <i>ATP3</i> | 1.87 | 2.94E-04 |
| | YPL078C | <i>ATP4</i> | 1.59 | 1.95E-03 |
| | YDR298C | <i>ATP5</i> | 1.28 | 7.69E-03 |
| | YKL016C | <i>ATP7</i> | 2.01 | 6.28E-04 |
| | YDL181W | <i>INH1</i> | 1.66 | 3.32E-04 |
| YJR077C | <i>MIR1</i> | 1.58 | 9.57E-06 | |
| Heme biosynthesis | YDR047W | <i>HEM12</i> | 1.29 | 3.58E-02 |
| | YOR176W | <i>HEM15</i> | 1.28 | 1.64E-03 |
| | YOR278W | <i>HEM4</i> | 1.31 | 3.34E-03 |
| Mitochondrial ribosome | YPR166C | <i>MRP2</i> | 1.42 | 2.11E-04 |
| | YDR405W | <i>MRP20</i> | 1.30 | 1.44E-02 |
| | YKL167C | <i>MRP49</i> | 1.21 | 3.06E-02 |
| | YKL142W | <i>MRP8</i> | 1.82 | 2.03E-02 |
| | YDL202W | <i>MRPL11</i> | 1.31 | 6.45E-08 |
| | YBL038W | <i>MRPL16</i> | 1.22 | 3.25E-02 |
| | YNL252C | <i>MRPL17</i> | 1.17 | 2.11E-02 |
| | YOR150W | <i>MRPL23</i> | 1.16 | 1.14E-02 |
| | YMR193W | <i>MRPL24</i> | 1.17 | 1.03E-02 |
| | YGR076C | <i>MRPL25</i> | 1.19 | 3.17E-03 |
| | YBR282W | <i>MRPL27</i> | 1.45 | 4.72E-05 |
| | YKL138C | <i>MRPL31</i> | 1.30 | 6.53E-03 |
| | YCR003W | <i>MRPL32</i> | 1.20 | 2.79E-02 |
| | YBR268W | <i>MRPL37</i> | 1.12 | 9.07E-03 |
| | YKL170W | <i>MRPL38</i> | 1.24 | 1.96E-02 |

Continued on following page

TABLE 2—Continued

| Function | Gene | | Increase in expression (fold) | P value |
|---------------------------------------|-----------------|-------------|-------------------------------|----------|
| | Systematic name | Common name | | |
| | YLR439W | MRPL4 | 1.25 | 1.53E-02 |
| | YDR337W | MRPS28 | 1.34 | 1.08E-04 |
| | YOR158W | PET123 | 1.13 | 2.55E-02 |
| mtDNA packaging | YMR072W | ABF2 | 1.79 | 1.04E-04 |
| | YJR144W | MGM101 | 1.69 | 3.12E-05 |
| Tricarboxylic acid cycle | YDR148C | KGD2 | 1.44 | 4.89E-03 |
| | YLR304C | ACO1 | 1.52 | 3.80E-03 |
| Retrograde signaling | YNL076W | MKS1 | 1.36 | 2.24E-05 |
| CCAAT-binding complex (GO:0016602) | YGL237C | HAP2 | 1.25 | 1.12E-04 |
| | YBL021C | HAP3 | 1.45 | 1.15E-06 |
| | YKL109W | HAP4 | 1.44 | 5.08E-03 |
| | YOR358W | HAP5 | 1.16 | 1.02E-02 |
| | YLR256W | HAP1 | 0.99 | 9.17E-01 |

sch9Δ mutant, we measured oxygen consumption rates in the *sch9Δ/sch9Δ* diploid and found that it consumes oxygen faster than the isogenic wild-type BY4743 cells, as predicted (Fig. 3B).

The *sch9Δ* mutant respiratory phenotype is dependent on Hap4p. We intersected the list of genes of the *sch9Δ* mutant that were highly significantly upregulated ($P < 0.001$) with ChIP/CHIP and with conserved *cis*-regulatory element data for all transcription factors available (http://fraenkel.mit.edu/yeast_map_2004/) (8, 14). Hap4p-bound intergenic regions and conserved CCAAT box elements were highly enriched upstream of genes whose expression was perturbed in *sch9Δ* cells (Table 3). Accordingly, we observed a modest but significant increase in expression of all CCAAT-binding factor subunits in the *sch9Δ* mutant (Tables 1 and 2; Fig. 1B). It thus seems likely that the CCAAT box-binding complex is influenced by *SCH9*. Since *HAP4* overexpression has been associated with an extended RLS, we investigated the role of *HAP4* in the *sch9Δ*

mutant. We first confirmed that the *hap4Δ* and *sch9Δ/hap4Δ* strains are unable to grow on nonfermentable carbon sources (data not shown). We then tested the effect of the *hap4Δ* mutation on the *sch9Δ* upregulation of respiratory genes and observed that it is reverted (Fig. 4A). Protein levels of many components of the electron transport chain and of the ATP synthase were decreased in the *sch9Δ/hap4Δ* mutant compared to the wild type (Fig. 4B). Increased oxygen consumption by *sch9Δ* cells was reverted by deletion of *HAP4* or of the cytochrome c_1 gene (*CYT1*) to levels close to that of a *rho*⁰ strain (Fig. 4C).

Increased life span of the *sch9Δ* mutant is partially dependent on increased respiration. As previously observed for CR cells, the *sch9Δ* mutation is associated with increased respiratory activity. We thus tested whether the CLS and RLS of the *sch9Δ* mutant are dependent on intact electron transport chain regulation or function. For this, we assessed the RLS of the

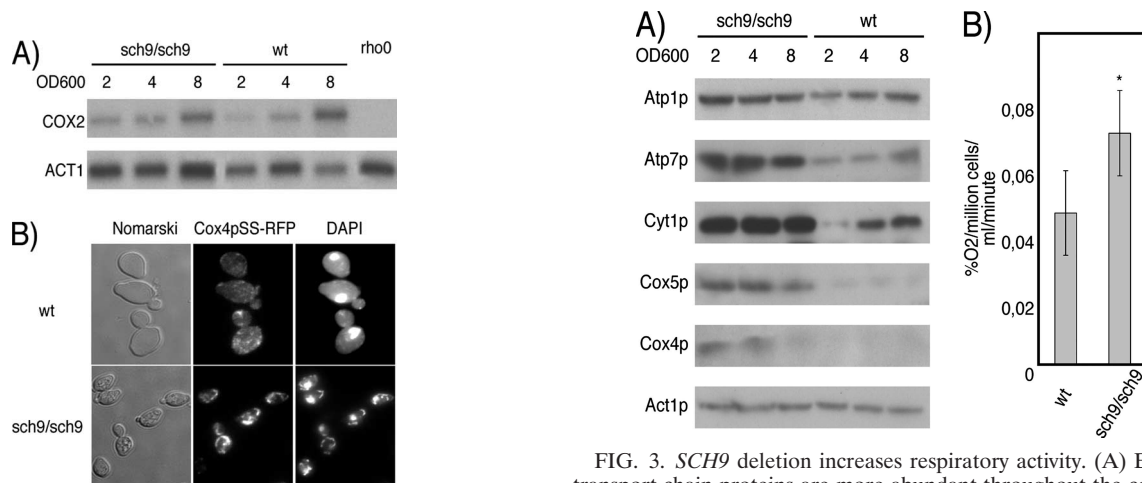


FIG. 2. mtDNA segregation is not affected in the *sch9Δ* mutant. (A) Southern blotting of mtDNA and a one-copy nuclear gene (*ACT1*). wt, wild type. (B) Mitochondrial morphology in the *sch9Δ* mutant observed by Cox4p-RFP localization and DAPI staining.

FIG. 3. *SCH9* deletion increases respiratory activity. (A) Electron transport chain proteins are more abundant throughout the course of culture growth in the *sch9Δ* strain. wt, wild type. (B) The oxygen consumption rate of the *sch9Δ/sch9Δ* mutant is significantly increased compared to that of the wild type (*, $P < 0.05$). Error bars indicate standard errors of the means.

TABLE 3. Transcription factors potentially regulating *sch9Δ*-dependent upregulated genes ($P < 1 \times 10^{-4}$)

| Transcription factor | Motif | P value | |
|----------------------|--------------|-----------------|--------------------|
| | | ChIP-CHIP bound | Motif conservation |
| <i>HAP4</i> | CCAAT | 1.35E-14 | 2.79E-05 |
| <i>HAP3</i> | CCAAT | 3.20E-04 | 2.79E-05 |
| <i>HAP2</i> | CCAAT | 2.84E-02 | 2.79E-05 |
| <i>HAP5</i> | CCAAT | NA ^a | 2.79E-05 |
| <i>HAP1</i> | CGGNNNNNNCGG | 5.91E-06 | 8.43E-06 |
| <i>SKN7</i> | ATTTGGCYG | 3.83E-01 | 6.78E-05 |
| | GSCC | | |
| <i>RGT1</i> | NA | NA | 8.54E-05 |

^a NA, not applicable.

sch9Δ mutant with or without *HAP4* and *CYT1*. A *hap4Δ* single mutant has essentially the same replicative longevity as the wild-type congenic strain, while the *sch9Δ* mutant and the *sch9Δ/hap4Δ* double mutant have significantly increased RLSs

($P = 1.8 \times 10^{-4}$ and $P = 8.2 \times 10^{-3}$, respectively) (Table 4; Fig. 5A). Similarly, the *sch9Δ* and *sch9Δ/cyt1Δ* mutants both show RLS extension compared to wild-type cells ($P = 4.4 \times 10^{-4}$ and $P = 8 \times 10^{-3}$, respectively) (Table 4), while we confirmed the previous finding that the *cyt1Δ* mutation causes a significant decrease in the RLS (Fig. 5B) (28). Since the effect of shutting down respiration in *sch9Δ* cells was small in terms of RLS, we tested whether the *hap4Δ* or *cyt1Δ* mutation could perturb the inability of the *sch9Δ* mutation to extend the CLS. As previously reported, we observed a dramatic extension of the CLS in the *sch9Δ* mutant (Fig. 5C and D). In contrast, the CLS of *hap4Δ* and *cyt1Δ* mutants was dramatically reduced compared to that of wild-type cultures, while the *sch9Δ/hap4Δ* and *sch9Δ/cyt1Δ* double mutants had slightly elongated CLSs compared to the *hap4Δ* and *cyt1Δ* single mutants (Fig. 5C and D). Interestingly, the *sch9Δ/hap4Δ* and *sch9Δ/cyt1Δ* double mutants fail to phenocopy *hap4Δ* and *cyt1Δ* mutants, respectively, in both CLS and RLS assays. Our data show that *sch9Δ* has respiration-independent effects on

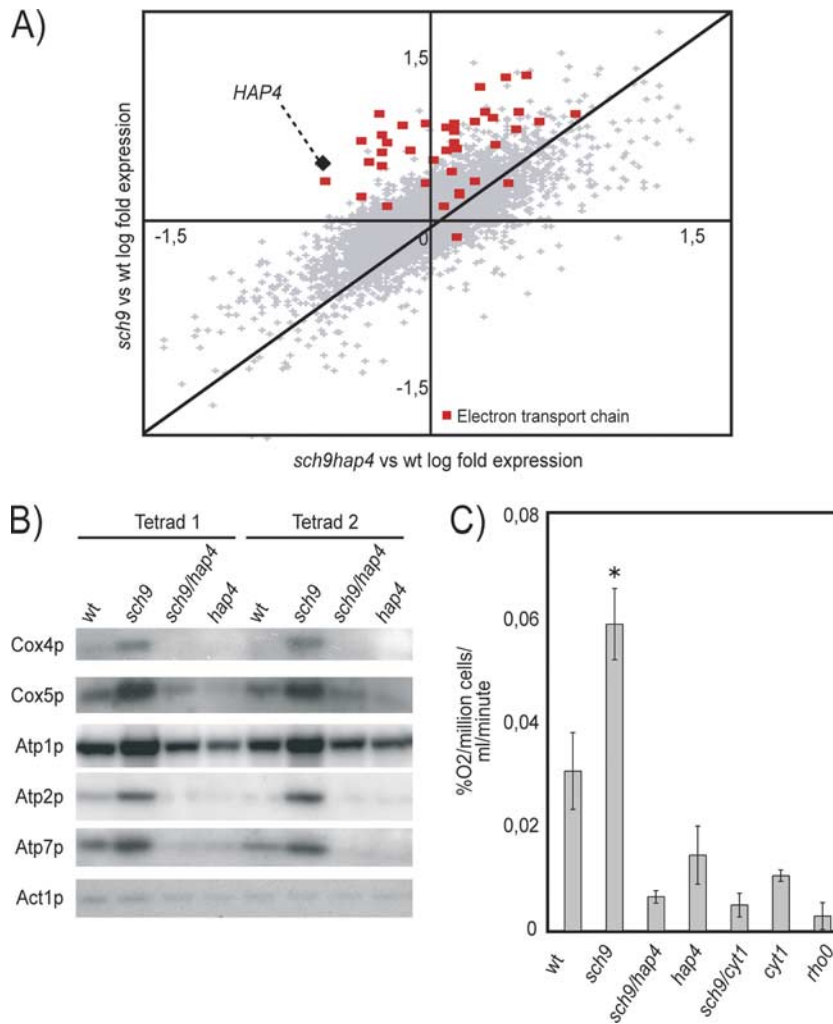


FIG. 4. The increased respiration of the *sch9Δ* mutant is *HAP4* and *CYT1* dependent. (A) Scatter plot comparing expression profiles obtained in microarray experiments with the *sch9Δ* mutant versus the wild type (wt) and with the *sch9Δ/hap4Δ* mutant versus the wild type. (B) The *sch9Δ* upregulation of mitochondrial electron transport chain proteins is reverted by deletion of *HAP4*. (C) Respiratory activity of the *sch9Δ* mutant is reverted by the *hap4Δ* and *cyt1Δ* mutations (*, $P < 0.001$). Error bars indicate standard errors of the means.

TABLE 4. Effect of HAP4 and CYT1 deletion on sch9 mutant life span

| Strain | Expt 1 | | Expt 2 | | Expt 3 | | P value |
|-------------------------|------------|----|-----------------|----|------------|----|---------|
| | Median RLS | n | Median RLS | n | Median RLS | n | |
| Wild type | 30 | 33 | 33 | 35 | 31 | 40 | 1 |
| <i>sch9</i> mutant | 45 | 42 | 47 | 35 | 48 | 40 | 1.8E-04 |
| <i>hap4</i> mutant | 34 | 34 | 29 | 35 | 29.5 | 40 | 7.5E-01 |
| <i>sch9 hap4</i> mutant | 37 | 46 | 38 | 33 | 38 | 40 | 8.2E-03 |
| Wild type | 36 | 22 | ND ^a | ND | 37 | 37 | 1 |
| <i>sch9</i> mutant | 44 | 25 | ND | ND | 46 | 40 | 4.4E-04 |
| <i>cyt1</i> mutant | 25 | 25 | ND | ND | 25 | 40 | 1.3E-05 |
| <i>sch9 cyt1</i> mutant | 46 | 23 | ND | ND | 45 | 40 | 8.0E-03 |

^a ND, not determined.

both the CLS and RLS. However, it seems that respiration or its proper regulation is required for full CLS extension in the *sch9Δ* mutant, while RLS extension by this mutation seems mostly respiration independent.

DISCUSSION

The *sch9Δ* mutation causes significant changes in expression of 643 genes, including a systematic increase in mitochondrial

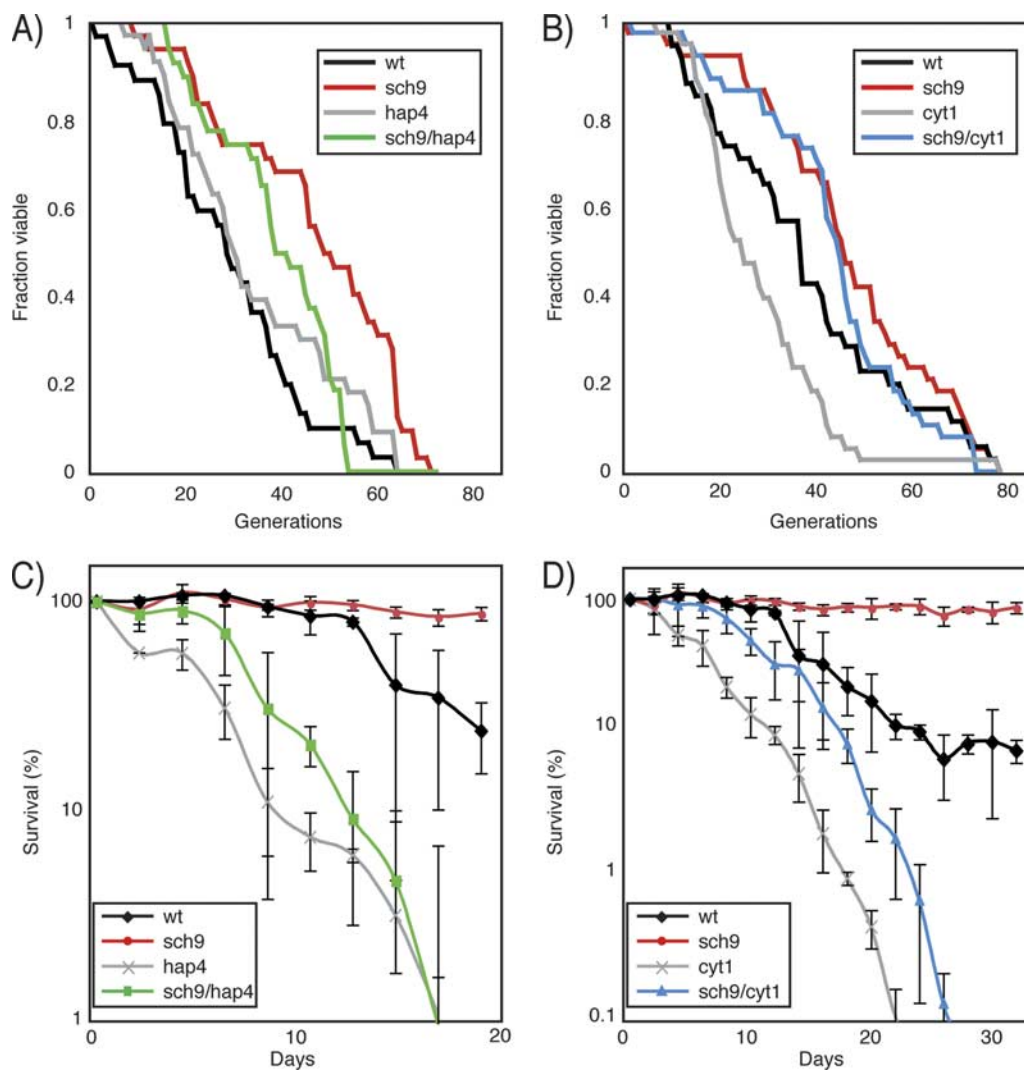


FIG. 5. The *sch9Δ* mutation increases CLS and RLS in a respiration-dependent manner. (A and B) The replicative longevity of the *sch9Δ* mutant is affected by the *hap4Δ* (A) and the *cyt1Δ* (B) deletions. wt, wild type. (C and D) The increased CLS of the *sch9Δ* mutant is blocked by deletion of *HAP4* (C) or *CYT1* (D). Error bars indicate standard errors of the means of three independent biological replicates.

TABLE 5. Stress response genes and other metabolic genes that are significantly modulated in the *sch9Δ* mutant ($P < 0.05$)

| Function | Systematic name | Common name | Increase in expression (fold) | <i>P</i> value |
|--------------------|-----------------|--------------|-------------------------------|----------------|
| Stress response | YHR008C | <i>SOD2</i> | 1.62 | 8.41E-03 |
| | YGL073W | <i>HSF1</i> | 1.13 | 3.25E-02 |
| | YFL014W | <i>HSP12</i> | 3.06 | 5.35E-03 |
| | YDR171W | <i>HSP42</i> | 1.71 | 3.96E-02 |
| | YFL016C | <i>MDJ1</i> | 1.46 | 8.56E-03 |
| | YNL064C | <i>YDJ1</i> | 1.44 | 3.16E-03 |
| Alcohol metabolism | YOL086C | <i>ADH1</i> | 1.13 | 2.62E-02 |
| | YMR303C | <i>ADH2</i> | 1.91 | 2.77E-03 |
| | YMR083W | <i>ADH3</i> | 1.54 | 4.72E-03 |

respiratory chain gene expression. Here, we have shown that mitochondrial activity of the *sch9Δ* mutant is increased. This finding was previously reported for CR yeast and in the *tor1Δ* strain (4).

Increasing respiration has drawbacks for cellular physiology by producing detrimental by-products such as reactive oxygen species (ROS) that limit the life span of cells in stationary-phase cultures, likely by oxidizing proteins, lipids, and nucleic acids (16). Besides ROS, ethanol also limits the CLS of yeast cells (9). Previous work has shown that the *sch9Δ* deletion causes an increase in heat and oxidative stress resistance, and *SOD2* was reported to be a downstream effector of the *sch9Δ* deletion increase in oxidative stress resistance and CLS (10, 12). Our expression profiling experiments show that many stress response genes are upregulated in *sch9Δ* cells (Table 5): we confirm increased expression of the mitochondrial superoxide dismutase gene *SOD2* and of several heat shock protein genes, and we show increased transcription of ethanol-degrading enzyme genes *ADH1*, -2, and -3. This provides additional molecular evidence for the *sch9Δ* mutant's resistance to stress and accelerated ethanol depletion (9).

Our study shows that not only is the *sch9Δ* mutant a genetic mimic of CR, but it also recapitulates many molecular hallmarks of CR in yeast. In fact, inactivation of *SCH9* provokes shunting of the fermentative metabolism of yeast to a more respirative mode and promotes the heat shock response and the turnover of ROS and alcohol. We find that a large part of the *SCH9* effect on the CLS is mediated by respiration, since deletion of *HAP4* or *CYT1* extensively abrogated *sch9Δ*-dependent extension of the CLS while RLS extension of *sch9Δ* was only slightly reduced by blocking respiration. Therefore, our data suggest that the *sch9Δ* mutation influences the CLS and RLS by both respiration-dependent and -independent mechanisms. Our data also indicate that the conditions required for extending the CLS and RLS are probably encountered by different means in the *sch9Δ* mutant, since disrupting respiration has a more dramatic effect on the CLS than on the RLS.

Our data support a recent finding that has challenged the relationship between CR-induced RLS extension and respiration (20). Those authors demonstrated that CR causes RLS extension in respiration-deficient yeast strains. Since *sch9Δ* is thought to be a CR genetic mimic and since it does not fully rely on respiration to promote CLS and RLS, our work further

weakens the evidence linking CR-induced RLS and increased respiration.

The respiration-independent effect of the *sch9Δ* mutation might be explained by it being resistant to oxidative and heat stress through increased ROS and ethanol turnover, which we detect in expression analysis of exponentially growing cultures. Thus, reduced production of detrimental by-products during the growth phase caused by a respirative metabolism and faster turnover of ethanol and ROS might lead to increased survival of the *sch9Δ* mutant during CLS analysis.

It is believed that Sch9p, Tor1p, and PKA kinases belong to highly integrated signaling pathways that are all involved in nutrient sensing (19, 24). *SCH9* and *TOR* inhibition increase CLS and RLS and are thought to mimic CR (23, 24). Recent findings show that Sch9p is the direct target of the TORC1 complex and that the *tor1Δ* strains display increased CLS and respiration (4, 38). This, in addition to our findings, supports the view that the TOR-*SCH9* pathway feeds into the regulation of respiration and that Sch9p might be one of the major effectors of TOR repression of respiratory activity, as it is the major effector of translational activation by the TOR pathway. The CCAAT box-binding complex (Hap2/3/4/5p) is a likely downstream effector of this nutrient-dependent signal transduction pathway. Hap4p was originally proposed to be the regulatory moiety of the CCAAT box-binding complex, and the TOR-*SCH9* pathway could thus reduce respiratory chain expression in high-glucose conditions by repressing Hap4p by a direct or indirect mechanism; in contrast, when glucose is depleted, decreased Sch9 signaling would induce the respiratory regulon as observed in our *sch9Δ* mutant (19).

It has been proposed that one of the major mitochondrial targets of TOR is translation (4). Here, we suggest that the TOR-*SCH9* pathway not only impinges on mitochondrial translation but also affects transcriptional activity of the nuclear respiratory regulon through Sch9p.

ACKNOWLEDGMENTS

We thank Mario Jolicoeur and Steve Hisiger for technical help with the oxygen consumption experiments. We thank Hervé Hogues for help with setting up a database for statistical analysis of gene ontology and transcription factor binding enrichment. We are grateful to Mike Tyers for providing the *sch9Δ* heterozygous mutant and the hemagglutinin-tagged Sch9 plasmid. Thanks go to Alexander Tzagolof for providing anti-Cyt1p, anti-Cox4p, and anti-Cox5p antibodies and to Jean Velours for anti-Atp1p, anti-Atp2p, and anti-Atp7p. The Cox4-RFP-expressing plasmid was provided by Benjamin Glick.

This work was supported by grants from the Canadian Institute for Health Research (CIHR). H.L. was supported by a CIHR fellowship. H.L. also acknowledges partial support from an NCIC and CNRC fellowship. This is NRCC publication 49523.

REFERENCES

- Ausubel, F. M., R. Brent, R. E. Kingston, D. D. Moore, J. G. Seidman, J. A. Smith, and K. Struhl. 1992. Current protocols in molecular biology. John Wiley and Sons, New York, NY.
- Barrientos, A., D. Pierre, J. Lee, and A. Tzagoloff. 2003. Cytochrome oxidase assembly does not require catalytically active cytochrome C. *J. Biol. Chem.* 278:8881-8887.
- Bevis, B. J., and B. S. Glick. 2002. Rapidly maturing variants of the Discosoma red fluorescent protein (DsRed). *Nat. Biotechnol.* 20:83-87.
- Bonawitz, N. D., M. Chatenay-Lapointe, Y. Pan, and G. S. Shadel. 2007. Reduced TOR signaling extends chronological life span via increased respiration and upregulation of mitochondrial gene expression. *Cell Metab.* 5:265-277.
- Bonawitz, N. D., M. S. Rodeheffer, and G. S. Shadel. 2006. Defective mitochondrial gene expression results in reactive oxygen species-mediated inhi-

- bition of respiration and reduction of yeast life span. *Mol. Cell. Biol.* **26**:4818–4829.
6. **Carlson, M., and D. Botstein.** 1982. Two differentially regulated mRNAs with different 5' ends encode secreted with intracellular forms of yeast invertase. *Cell* **28**:145–154.
 7. **Chen, X. J., X. Wang, B. A. Kaufman, and R. A. Butow.** 2005. Aconitase couples metabolic regulation to mitochondrial DNA maintenance. *Science* **307**:714–717.
 8. **Cliften, P., P. Sudarsanam, A. Desikan, L. Fulton, B. Fulton, J. Majors, R. Waterston, B. A. Cohen, and M. Johnston.** 2003. Finding functional features in Saccharomyces genomes by phylogenetic footprinting. *Science* **301**:71–76.
 9. **Fabrizio, P., C. Gattazzo, L. Battistella, M. Wei, C. Cheng, K. McGrew, and V. D. Longo.** 2005. Sir2 blocks extreme life-span extension. *Cell* **123**:655–667.
 10. **Fabrizio, P., L. L. Liou, V. N. Moy, A. Diaspro, J. Selverstone Valentine, E. B. Gralla, and V. D. Longo.** 2003. SOD2 functions downstream of Sch9 to extend longevity in yeast. *Genetics* **163**:35–46.
 11. **Fabrizio, P., and V. D. Longo.** 2003. The chronological life span of *Saccharomyces cerevisiae*. *Aging Cell* **2**:73–81.
 12. **Fabrizio, P., F. Pozza, S. D. Pletcher, C. M. Gendron, and V. D. Longo.** 2001. Regulation of longevity and stress resistance by Sch9 in yeast. *Science* **292**:288–290.
 13. **Gietz, R. D., and R. A. Woods.** 2002. Transformation of yeast by lithium acetate/single-stranded carrier DNA/polyethylene glycol method. *Methods Enzymol.* **350**:87–96.
 14. **Harbison, C. T., D. B. Gordon, T. I. Lee, N. J. Rinaldi, K. D. Macisaac, T. W. Danford, N. M. Hannett, J. B. Tagne, D. B. Reynolds, J. Yoo, E. G. Jennings, J. Zeitlinger, D. K. Pokholok, M. Kellis, P. A. Rolfe, K. T. Takusagawa, E. S. Lander, D. K. Gifford, E. Fraenkel, and R. A. Young.** 2004. Transcriptional regulatory code of a eukaryotic genome. *Nature* **431**:99–104.
 15. **Hoffman, C. S., and F. Winston.** 1987. A ten-minute DNA preparation from yeast efficiently releases autonomous plasmids for transformation of *Escherichia coli*. *Gene* **57**:267–272.
 16. **Jazwinski, S. M.** 2005. Yeast longevity and aging—the mitochondrial connection. *Mech. Ageing Dev.* **126**:243–248.
 17. **Jiang, J. C., E. Jaruga, M. V. Repnevskaya, and S. M. Jazwinski.** 2000. An intervention resembling caloric restriction prolongs life span and retards aging in yeast. *FASEB J.* **14**:2135–2137.
 18. **Jorgensen, P., J. L. Nishikawa, B. J. Breitkreutz, and M. Tyers.** 2002. Systematic identification of pathways that couple cell growth and division in yeast. *Science* **297**:395–400.
 19. **Jorgensen, P., I. Rupes, J. R. Sharom, L. Schneper, J. R. Broach, and M. Tyers.** 2004. A dynamic transcriptional network communicates growth potential to ribosome synthesis and critical cell size. *Genes Dev.* **18**:2491–2505.
 20. **Kaerberlein, M., D. Hu, E. O. Kerr, M. Tsuchiya, E. A. Westman, N. Dang, S. Fields, and B. K. Kennedy.** 2005. Increased life span due to caloric restriction in respiratory-deficient yeast. *PLoS Genet.* **1**:e69.
 21. **Kaerberlein, M., and B. K. Kennedy.** 2005. Large-scale identification in yeast of conserved ageing genes. *Mech. Ageing Dev.* **126**:17–21.
 22. **Kaerberlein, M., K. T. Kirkland, S. Fields, and B. K. Kennedy.** 2004. Sir2-independent life span extension by caloric restriction in yeast. *PLoS Biol.* **2**:E296.
 23. **Kaerberlein, M., K. T. Kirkland, S. Fields, and B. K. Kennedy.** 2005. Genes determining yeast replicative life span in a long-lived genetic background. *Mech. Ageing Dev.* **126**:491–504.
 24. **Kaerberlein, M., R. W. Powers, 3rd, K. K. Steffen, E. A. Westman, D. Hu, N. Dang, E. O. Kerr, K. T. Kirkland, S. Fields, and B. K. Kennedy.** 2005. Regulation of yeast replicative life span by TOR and Sch9 in response to nutrients. *Science* **310**:1193–1196.
 25. **Kraakman, L., K. Lemaire, P. Ma, A. W. Teunissen, M. C. Donaton, P. Van Dijk, J. Winderickx, J. H. de Winde, and J. M. Thevelein.** 1999. A *Saccharomyces cerevisiae* G-protein coupled receptor, Gpr1, is specifically required for glucose activation of the cAMP pathway during the transition to growth on glucose. *Mol. Microbiol.* **32**:1002–1012.
 26. **Lamboursain, L., F. St-Onge, and M. Jolicoeur.** 2002. A lab-built respirometer for plant and animal cell culture. *Biotechnol. Prog.* **18**:1377–1386.
 27. **Lin, S. J., P. A. Defossez, and L. Guarente.** 2000. Requirement of NAD and SIR2 for life-span extension by caloric restriction in *Saccharomyces cerevisiae*. *Science* **289**:2126–2128.
 28. **Lin, S. J., M. Kaerberlein, A. A. Andalis, L. A. Sturtz, P. A. Defossez, V. C. Culotta, G. R. Fink, and L. Guarente.** 2002. Calorie restriction extends *Saccharomyces cerevisiae* lifespan by increasing respiration. *Nature* **418**:344–348.
 29. **Lorenz, M. C., X. Pan, T. Harashima, M. E. Cardenas, Y. Xue, J. P. Hirsch, and J. Heitman.** 2000. The G protein-coupled receptor gpr1 is a nutrient sensor that regulates pseudohyphal differentiation in *Saccharomyces cerevisiae*. *Genetics* **154**:609–622.
 30. **Martchenko, M., A. M. Alarco, D. H Marcus, and M. Whiteway.** 2004. Super-oxide dismutases in *Candida albicans*: transcriptional regulation and functional characterization of the hyphal-induced SOD5 gene. *Mol. Biol. Cell* **15**:456–467.
 31. **Meeusen, S., Q. Tieu, E. Wong, E. Weiss, D. Schieltz, J. R. Yates, and J. Nunnari.** 1999. Mgm101p is a novel component of the mitochondrial nucleoid that binds DNA and is required for the repair of oxidatively damaged mitochondrial DNA. *J. Cell Biol.* **145**:291–304.
 32. **Piper, P. W., N. L. Harris, and M. MacLean.** 2006. Preadaptation to efficient respiratory maintenance is essential both for maximal longevity and the retention of replicative potential in chronologically ageing yeast. *Mech. Ageing Dev.* **127**:733–740.
 33. **Powers, R. W., III, M. Kaerberlein, S. D. Caldwell, B. K. Kennedy, and S. Fields.** 2006. Extension of chronological life span in yeast by decreased TOR pathway signaling. *Genes Dev.* **20**:174–184.
 34. **Roelants, F. M., P. D. Torrance, and J. Thorner.** 2004. Differential roles of PDK1- and PDK2-phosphorylation sites in the yeast AGC kinases Ypk1, Pkc1 and Sch9. *Microbiology* **150**:3289–3304.
 35. **Sato, H., A. Tachifuji, M. Tamura, and I. Miyakawa.** 2002. Identification of the YMN-1 antigen protein and biochemical analyses of protein components in the mitochondrial nucleoid fraction of the yeast *Saccharomyces cerevisiae*. *Protoplasma* **219**:51–58.
 36. **Sobko, A.** 2006. Systems biology of AGC kinases in fungi. *Sci. STKE* **2006**:re9.
 37. **Toda, T., S. Cameron, P. Sass, and M. Wigler.** 1988. SCH9, a gene of *Saccharomyces cerevisiae* that encodes a protein distinct from, but functionally and structurally related to, cAMP-dependent protein kinase catalytic subunits. *Genes Dev.* **2**:517–527.
 38. **Urban, J., A. Souillard, A. Huber, S. Lippman, D. Mukhopadhyay, O. DeLoche, V. Wanke, D. Anrather, G. Ammerer, H. Riezman, J. R. Broach, C. De Virgilio, M. N. Hall, and R. Loewith.** 2007. Sch9 is a major target of TORC1 in *Saccharomyces cerevisiae*. *Mol. Cell* **26**:663–674.
 39. **Winzler, E. A., D. D. Shoemaker, A. Astromoff, H. Liang, K. Anderson, B. Andre, R. Bangham, R. Benito, J. D. Boeke, H. Bussey, A. M. Chu, C. Connelly, K. Davis, F. Dietrich, S. W. Dow, M. El Bakkoury, F. Foury, S. H. Friend, E. Gentalen, G. Giaever, J. H. Hegemann, T. Jones, M. Laub, H. Liao, N. Liebundguth, D. J. Lockhart, A. Lucau-Danila, M. Lussier, N. M'Rabet, P. Menard, M. Mittmann, C. Pai, C. Rebischung, J. L. Revuelta, L. Riles, C. J. Roberts, P. Ross-MacDonald, B. Scherens, M. Snyder, S. Sookhai-Mahadeo, R. K. Storms, S. Veronneau, M. Voet, G. Volckaert, T. R. Ward, R. Wysocki, G. S. Yen, K. Yu, K. Zimmermann, P. Philippsen, M. Johnston, and R. W. Davis.** 1999. Functional characterization of the *S. cerevisiae* genome by gene deletion and parallel analysis. *Science* **285**:901–906.
 40. **Xue, Y., M. Batlle, and J. P. Hirsch.** 1998. GPR1 encodes a putative G protein-coupled receptor that associates with the Gpa2p Galpha subunit and functions in a Ras-independent pathway. *EMBO J.* **17**:1996–2007.
 41. **Zelenaya-Troitskaya, O., S. M. Newman, K. Okamoto, P. S. Perlman, and R. A. Butow.** 1998. Functions of the high mobility group protein, Abf2p, in mitochondrial DNA segregation, recombination and copy number in *Saccharomyces cerevisiae*. *Genetics* **148**:1763–1776.